3D Thermo-Electro-Mechanical Simulations of Gas Sensors Based on SOI Membranes

Chih-Cheng Lu [*], D. Setiadi [*], F. Udrea [*], W.I. Milne [*], J.A. Covington [**], J.W. Gardner [**]

[*] Department of Engineering, University of Cambridge, Cambridge CB2 1PZ, UK, ccl23@eng.cam.ac.uk

[**] School of Engineering, University of Warwick, Coventry CV4 7AL, UK, esjwg@eng.warwick.ac.uk

ABSTRACT

3D thermo-electro-mechanical device simulations are presented of a novel fully CMOS-compatible MOSFET gas sensor operating in a SOI membrane. A comprehensive stress analysis of a Si-SiO_2–based multilayer membrane has been performed to ensure a high degree of mechanical reliability at a high operating temperature (e.g. up to 400°C). Moreover, optimisation of the layout dimensions of the SOI membrane, in particular the aspect ratio between the membrane length and membrane thickness, has been carried out to find the best trade-off between minimal device power consumption and acceptable mechanical stress.

Keywords: solid-state gas sensors, electro-thermal-mechanical simulations, SOI devices, multilayer membrane, and device optimization.

1. INTRODUCTION

Solid state gas sensors have been widely used in industrial applications and environmental control for several decades. In particular, chemoresistors are the simplest form of all gas sensors [1]. Chemoresistive sensors are based on sensing materials, such as SnO_2 or ZnO, that react at high temperatures with certain atmospheric gases and hence change their electrical conductivity. More complex sensors, such as FET based chemical sensors with a catalytic palladium gate [2], have also been reported to be sensitive to hydrogen. Their use has been recently extended to the detection of other gases and even odours, however, their commercial success has yet to be proven.

The general requirements for solid-state sensors are low power consumption, high sensitivity and a simple, inexpensive fabrication process. Silicon technology and micro-machining techniques offer the possibility of low-cost fabrication and potential CMOS integration. However the temperature range of standard CMOS technology is limited and integration is difficult to realise when non-standard CMOS steps, such as platinum heater formation, are required. Nevertheless designs which make of platinum heaters embedded within a low-stress silicon nitride membrane [3] have been successfully developed. Recently, Gardner and Udrea have proposed novel MOSFET gas sensors based on silicon-on-insulator (SOI) technology that can operate at relatively high temperatures [4,5] and are fully CMOS compatible. The MOSFETs are implemented within a SOI membrane and act as heaters through the self-heating effect. These sensors can offer very low power consumption, while the fabrication process is fully compatible with the current SOI CMOS or Bi-CMOS technology.

2. SENSOR STRUCTURE

Chemoresistive gas sensors with MOSFET heaters are fabricated on a 1~3 μm thick SOI square membrane, formed by using an anisotropic KOH etching of the silicon substrate, as shown in Fig. 1. The sensing element is represented here as a 10-μm thick SnO_2 film located above the heater and isolated from it through an oxide passivation layer. The active SOI layer is a lightly boron-doped p-type <100> silicon layer. The thin insulating layer (buried oxide) serves a dual purpose: (1) it acts as an etch stop and thermally isolates the membrane to allow high temperatures to develop in the sensing area; (2) it provides an effective electrical isolation between individual devices or circuits placed outside the membrane area [5]. A local oxidation is grown surrounding a MOSFET heater is used for lateral electrical and thermal isolations within the membrane area.

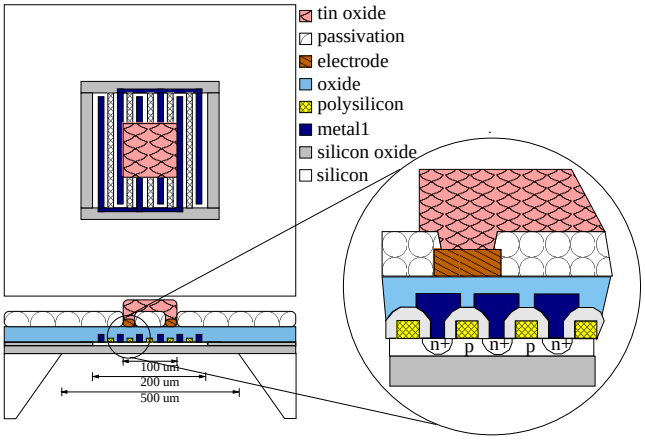

Fig. 1 Schematic diagram of a SOI MOSFET gas sensor.

3. SIMULATIONS AND RESULTS

3.1 Electrothermal Simulations

Electrothermal simulations of solid-state sensors have been previously reported in [3,6-8]. The electrical power generated in the heater is thermally via the membrane and surrounding atmosphere. The electrical power consumption equates with the total thermal losses. Both conduction and free convection losses are taken into account but radiation loss can be neglected below 400 °C. A semi-empirical

second-order model can be used to describe the power dissipation in a high temperature gas-sensor [3]:

$$P_H = \alpha_P (T_H - T_a) + \beta_P (T_H - T_a)^2 \quad (1)$$

where P_H is the heater power, T_H-T_a is the temperature difference between the operating and ambient temperatures, and α_P and β_P are the thermal loss coefficients determined experimentally.

Electrothermal simulations have been performed using the SOLIDIS-ISE© simulator, which is designed to deal with coupled physical interactions on microstructures [9]. In our particular design, the heater consists of a MOSFET operating in the forward regime. The power generated by the MOSFET depends on its source-drain voltage drop V_{ds}, the drain current I_{ds} and can be adjusted via the MOS gate voltage.

As mentioned before, the electrical power P_E, is converted into heat so we can write:

$$P_E = I_{DS} V_{DS} = P_H \quad (2)$$

where P_H is given in equation (1).

The simulator uses coupled current-lattice temperature models as well as scattering mobility models that can account for the MOSFET channel mobility degradation at high temperatures (580~640 K) as shown in Fig. 2(a). The temperature in the active area is observed to increase almost linearly with applied gate voltage once a threshold voltage of 0.7 V has been achieved. This is an important finding since adjusting and driving the heater at a desired temperature can be easily estimated from the gate voltage. Fig. 2(b) gives the applied gate voltage vs. temperature as well as the power consumption in 2D simulation.

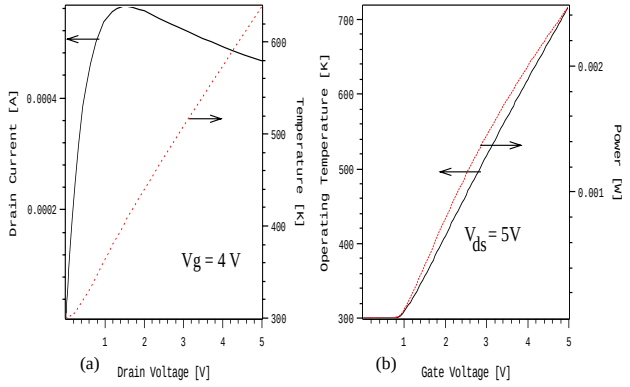

Fig. 2 (a) Forward I-V characteristic and lattice temperature elevation. (b) Gate voltage vs. temperature and power.

Numerical simulations show that the shape of the MOSFET micro-heaters has an important effect on the temperature distribution profile and in particular the uniformity of the temperature in the sensing area. While several designs have been considered, this study is limited to an interdigitated design with a heater area of (200μm×200μm) that gives reasonable thermal and electrical characteristics. The 3D cross-sectional temperature profile within the sensing area for this particular interdigitated design is shown in Fig. 3(a). The membrane area (500μm×500μm) is considerably larger than the heater area to provide effective thermal insulation and prevent heat dissipation from the IC area, outside the membrane. Therefore it is possible to operate the drive/processing circuits close to the room temperature in spite of very high temperatures present in the sensing area, as shown in Fig. 3(b).

3.2 Thermomechanical Simulations

A comprehensive thermomechanical study of the SOI MOSFET gas sensors has also been carried out. The thickness of the SOI membrane will greatly impact upon the manufacturing yield of the device. In addition the lifetime of these sensors may be considerably shortened by mechanical rupture of the membrane - especially when operated at high temperatures. In particular silicon oxide has been shown to be more brittle, and therefore less mechanically robust, than silicon in spite of its low thermal conductivity. A thick membrane is expected to have an improved mechanical reliability but on the other hand leads to higher power losses.

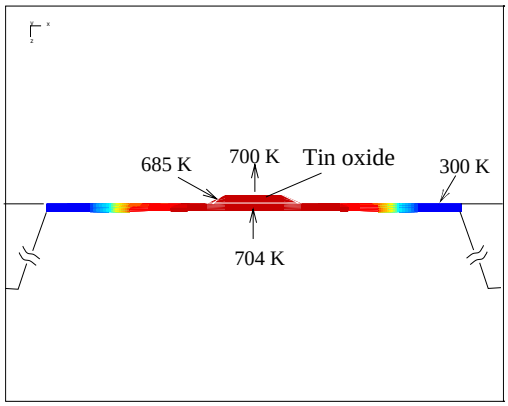

(a)

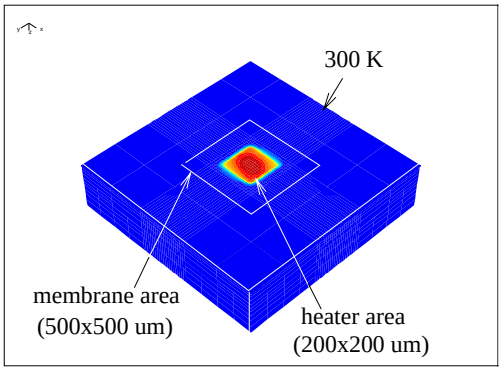

(b)

Fig. 3 (a) A cross-sectional temperature profile of the sensing element on the membrane. (b) A temperature profile from a plan view.

Based on the assumptions of classic thin-plate theory [10], the in-plane principal stress can be obtained from:

$$\sigma_1 = \frac{Eu^2}{3(1-\upsilon^2)}\left(\frac{l}{h}\right)^2, \sigma_2 = \frac{q}{2}\left(\frac{l}{h}\right)^2 \psi_1(u) \quad (3)$$

where $\psi_1(u) = \frac{3(u - \tanh u)}{u^2 \tanh u}$, and $u^2 = \frac{l^2 S}{4D}$.

l: the length of a square membrane
h: thickness of a membrane
q: load pressure.
S: a parameter from experimental data.

Let $D = \frac{-E h^3}{12(1-\upsilon^2)}$, which is the flexural rigidity of a thin plate. *E* is Young's modulus and *v* is Poisson's ratio. Thus:

$$\sigma_{max} = \sigma_1 + \sigma_2 \quad (4)$$

It is very important to note that the maximum stress σ_{max} is a function of the load pressure *q* and the aspect ratio *l*/*h*. By changing the load pressure, the maximum stress (i.e. the principal stress) can be derived for various values of *l*/*h*. According to previously reported experimental results [10], the maximum stress increases with a larger *l*/*h* ratio in a membrane made of isotropic and homogeneous material.

Since our sensor membrane operates at very high temperatures, the thermal stress induced by such temperatures should be considered carefully. However, neither the residual stress nor intrinsic stress is considered in the simulator at present. In fact residual stress can be reduced by controlling doping concentration and intrinsic stress is highly dependent on the SOI process used and varies considerably from one technique (e.g. SIMOX) to the other (e.g. wafer bonding).

A 500μm×500μm SOI membrane area comprised of Si and SiO_2 layers with a thickness ratio of 1:2 has been simulated to optimise the heat transfer and mechanical characteristics. In order to do this a cubic solid model of the SOI substrate with a square membrane is constructed. The boundary conditions applied to the micromechanical simulation are: (a) the edges of the membrane and the substrate base of the sensor are clamped, and thus the displacements are assumed zero; (b) the temperature along the silicon substrate base is given by the ambient temperature; (c) free convective exchange with the surrounding ambient atmosphere on the upper and lower surfaces of the membrane is considered.

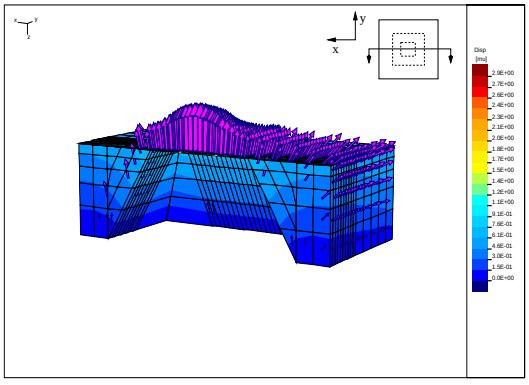

Fig. 4 A result of 3D deformation at 670 K with the aspect ratio *l*/*h* =250. (Arrows represent spatial displacement vectors)

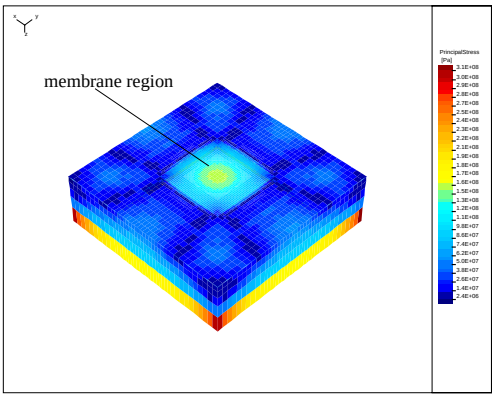

Fig. 5 A 3D simulation of the maximum stress at 670 K with the aspect ratio *l*/*h* =250.

Simulated schematic results illustrating the upward deformation (-Z direction) and the maximum stress distribution profile are shown in Fig. 4 and Fig. 5. Compressive stress in the active silicon layer and tensile stress in the buried oxide layer have been observed as seen in Fig. 6. The resultant magnitude of maximum stress in membrane area increases dramatically with the operating temperature, for example, from 65 MPa at room temperature to 255 MPa at 700 K. The maximum stress versus the operating temperature for different *l*/*h* ratios is shown in Fig. 7. It can be noticed that the maximum stress increases linearly with a larger *l*/*h* ratio value above 500 K, except for the curve with the *l*/*h* ratio of 200, exhibiting fluctuating characteristic compared to the other results. The material property constants employed for thermo-mechanical simulations are listed in Table 1.

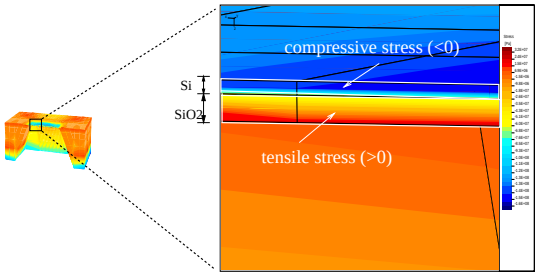

Fig. 6 Stress illustration of SOI membrane at a high temperature of 700 K.

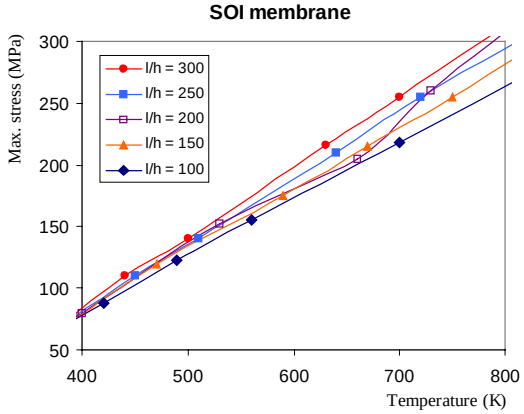

Fig. 7 Variation of the maximum stress in the SOI membrane with the operating temperature.

4. OPTIMIZATION OF SENSOR DESIGN

The design criteria to assess the general performance and considerations of the sensor are given below:

1. Reduced maximum stress in both Si and SiO_2 membrane layers, in particular in the heated active area (central part of the membrane).
2. Uniform temperature distribution over the sensing element (a 100μm×100μm area).
3. Low power consumption (relatively small heating area and thin membrane).
4. Large sensing area for high sensitivity

According to the above criteria extensive numerical simulations have been carried out to evaluate the performance of the sensor. Selected results are summarised in Table 2. Design A suffers from the highest power consumption and large variation in the temperature while offering the best mechanical stability in maximum stress and deflection. Design B shows a significant drop in power consumption though the maximum stress and the variation in the temperature are slightly improved. Design D benefits from much lower power consumption and better temperature homogeneity. Design E exhibits the lowest power consumption and temperature homogeneity, but unfortunately exhibits a significantly increased maximum stress. Design C is disregarded in the evaluation because of the fluctuating stress by comparison to the other designs. As a result, design D with the aspect ratio of 250 and thus a 2-μm thick SOI membrane is cautiously selected as offering the best trade-off with the maximum compressive stress of 240 MPa, the maximum deflection of 3.1 μm upwards and relatively low power consumption of about 36 mW at 700K. Nevertheless the choice of an optimal design may vary with different criteria and priorities for sensor specification.

Physical parameters	**Si**	**SiO_2**
Young's modulus (E, GPa)	190	73
Poisson's ratio (ν)	0.22	0.15
Thermal conductivity (k,$Wm^{-1}°C^{-1}$)	157	1.4
Thermal expansion coefficient (α, K^{-1})	2.33e-6	0.55e-6

Table 1 The physical constants employed in SOLIDIS-ISE simulator [1,6].

Square SOI membranes: l (length of membrane) = 500 μm	**A** l/h = 100	**B** l/h = 150	**C** l/h = 200	**D** L/h = 250	**E** l/h = 300
Maximum stress (Mpa)	-220	-228	-235	-240	-255
Maximum deflection (μm)	2.6	2.8	2.9	3.1	3.2
Maximum relative temperature variation (%)	2.6	2.2	1.8	1.4	1.2
Power consumption (mW)	53	44	39	36	34

Table 2 Optimal evaluation for a microsensor with a SOI membrane.

5. CONCLUSIONS

In this paper a study of SOI microsensors suspended on a relatively thin membrane has been carried out using advanced 3D numerical simulations. The results reveal that a new generation of chemoresistive gas sensors is possible possessing lower power consumption, acceptable mechanical stability and uniform temperature distribution. By carefully optimising the ratio between membrane length and membrane thickness one can predict the maximum stress and the power consumption for the sensor. An optimal layout and geometrical design is found through numerical simulations to offer a good trade-off between the thermo-electro-mechanical characteristics. However, it should be emphasised that this prediction is greatly dependent on the choice of the physical constants and in particular material properties determined by various CMOS process. Careful attention has been paid in selecting these parameters and a further experimental demonstration is necessary to verify the validity of the simulation.

REFERENCES

[1] J.W. Gardner, "Microsensors principles and applications", Wiley, 1994.

[2] I. Lundstrom et al., "A hydrogen sensitive MOS field-effect transistor", Appl. Phys. Lett., 26, pp55-57, 1975.

[3] A. Pike and J.W. Gardner, "Thermal modelling and characterisation of micropower chemoresistive silicon sensors", Sensors and Actuators, B, 45, pp19-26, 1997.

[4] F. Udrea and J.W. Gardner, UK and World patent application GB2321336A and WO98/32009.

[5] J.W. Gardner, F. Udrea, W.I. Milne, "Numerical simulation of a new generation of high-temperature, micropower and odour sensors based on SOI technology", Proc. of SPIE Smart Electronics and MEMS, Vol. 3673, pp104-112, March 1999.

[6] S. Astie, A.M. Gue *et al.*, "Optimization of an integrated SnO2 gas sensor using a FEM simulator", Sensors and Actuators, A, 69, pp205-211, 1998.

[7] F. Udrea and J.W. Gardner, "Design of a silicon microsensor array device for gas analysis", Microelectronics Journal, 27, pp449-457, 1996.

[8] D. Setiadi, F. Udrea et al, "3D numerical simulation of novel SOI MOSFET based gas sensors", Proc. of Chemical Sensors IV, The Electrochemical Soc., pp416-419, Oct. 1999.

[9] ISE TCAD, " SOLIDIS-ISE 5.0 manual", Zurich, Switzerland, 1998.

[10] S. Timoshenko and S. Woinowski-Krieger, "Theory of plates and shells", McGraw-Hill, pp13-20, 1959.